Susceptibility of Cholangiocarcinoma Cells to Parthenolide-Induced Apoptosis

Jong-Hyun Kim,[1] Lan Liu,[1] Seung-Ok Lee,[1] Yong-Tae Kim,[2] Kyung-Ran You,[1] and Dae-Ghon Kim[1]

[1]Division of GI and Hepatology, Department of Internal Medicine, Institute for Molecular Biology and Genetics, Chonbuk National University Medical School and Hospital, Jeonju, Jeonbuk and [2]Department of Internal Medicine, Seoul National University School of Medicine, Seoul, Republic of Korea

Abstract

Cholangiocarcinomas are intrahepatic bile duct carcinomas that are known to have a poor prognosis. Sesquiterpene lactone parthenolide, which is the principal active component in medicinal plants, has been used to treat tumors. Parthenolide effectively induced apoptosis in all four cholangiocarcinoma cell lines in a dose-dependent manner. However, the sarcomatous SCK cells were more sensitive to parthenolide than the other adenomatous cholangiocarcinoma cells. Therefore, this study investigated whether or not the expression of p53, the *Fas*/Fas ligand (*FasL*), Bcl-2/Bcl-X_L determines the enhanced drug susceptibility of SCK cells. The results showed that Bcl-2 family molecules, such as Bid, Bak, and Bax, are involved in the parthenolide-induced apoptosis and that the defective expression of Bcl-X_L might contribute to the higher parthenolide sensitivity in the SCK cells than in the other adenomatous cholangiocarcinoma cells. SCK cells, which stably express Bcl-X_L, were resistant to parthenolide, whereas Bcl-X_L-positive Choi-CK cells transfected with the antisense Bcl-X_L showed a higher parthenolide sensitivity than the vector control cells. Molecular dissection revealed that Bcl-X_L inhibited the translocation of Bax to the mitochondria, decreased the generation of intracellular reactive oxygen species, reduced the mitochondrial transmembrane potential ($\Delta\Psi_m$), decreased the release of cytochrome *c*, decreased the cleavage of poly(ADP-ribose) polymerase, and eventually inhibited apoptotic cell death. These results suggest that parthenolide effectively induces oxidative stress-mediated apoptosis, and that the susceptibility to parthenolide in cholangiocarcinoma cells might be modulated by Bcl-X_L expression in association with Bax translocation to the mitochondria. (Cancer Res 2005; 65(14): 6312-20)

Introduction

Cholangiocarcinomas are malignant tumors that are derived from the bile duct epithelium. They are quite prevalent in some areas of Southeast Asia where liver fluke infestations are endemic. Cholangiocarcinomas account for 77% of all primary liver tumors (1). Chronic biliary tract inflammations resulting from bacterial infections, parasitic infestations, or chronic inflammatory diseases of the biliary tract (such as primary sclerosing cholangitis) are significant risk factors for the development of cholangiocarcinomas. The prognosis for cholangiocarcinoma patients is quite poor due to the lack of an early diagnosis and the fact that the tumor is relatively resistant to chemotherapy (2–4). At the time of the diagnosis, ~70% of cholangiocarcinoma patients have an occult metastasis or advanced local disease, which precludes a curative resection. Even the 30% of patients who are candidates for a curative resection develop recurrent disease at either the anastomotic site or within the intrahepatic biliary tree, and succumb due to the progression of the disease or cholangitis (5). Generally, chemotherapeutic drugs exert their antitumor effects by inducing apoptosis in cancer cells. Therefore, in order to improve the therapeutic modalities and to develop alternative treatments, new agents that induce apoptosis need to be identified and their mechanism(s) of action need to be investigated. Recently, four cholangiocarcinoma cell lines were isolated and cytogenetically characterized (6). The molecular characteristics of the four cholangiocarcinoma cell lines were further investigated and their chemosensitivities were examined.

Sesquiterpene lactones have been widely used in indigenous medical practice, including the treatment of migraines (7, 8), inflammation (9, 10), and tumors (11, 12). Parthenolide, which is the major sesquiterpene lactone found in medicinal plants such as feverfew (*Tanacetum parthenium*), is known to inhibit interleukin-1 and tumor necrosis factor-α-mediated nuclear factor κB activation, which is responsible for its antiinflammatory activity (13, 14). Because of their low potencies, there have been few studies on the cytotoxic and antitumor effects of the sesquiterpene lactones. However, it was recently reported that parthenolide inhibits the *in vitro* growth of tumor cells in a cytostatic manner and might represent a new class of cancer chemotherapeutic drugs (15). Previously, it was reported that parthenolide has effective anticancer effects including the induction of apoptosis and growth arrest in sarcomatous hepatocellular carcinoma cells, and that oxidative stress might contribute to the parthenolide-induced apoptosis in a glutathione-sensitive manner (15). Therefore, the aim of this study was to determine if parthenolide effectively induces apoptosis and whether this apoptogenic effect is modulated by the biological characteristics or by genetic alterations in the cholangiocarcinoma cells. Interestingly, the susceptibility to parthenolide was observed in all the cholangiocarcinoma cell lines. Moreover, it was higher in the Bcl-X_L-defective cholangiocarcinoma cells than in the Bcl-X_L-positive cholangiocarcinoma cells. This suggests that parthenolide-mediated oxidative stress and the concomitant involvement of the Bcl-2 family molecules might play a major role in the apoptogenic effect.

Materials and Methods

Cell culture, transfection, and apoptosis assay. Four distinct cholangiocarcinoma cell lines (SCK, JCK, Cho-CK, and Choi-CK) were cultured and treated with 10 μmol/L (or other concentrations as noted) parthenolide (dissolved in either DMSO or absolute alcohol) in DMEM

Requests for reprints: Dae-Ghon Kim, Division of GI and Hepatology, Chonbuk National University Medical School and Hospital, 634-18 Keumam-dong, Dukjin-ku, Jeonju, Jeonbuk 561-712, Republic of Korea. Phone: 82-63-250-1681; Fax: 82-63-254-1609; E-mail: daeghon@moak.chonbuk.ac.kr.

supplemented with 10% fetal bovine serum in air containing 5% CO_2. The lung cancer (A549 and NCIH522), colon cancer (HCT116 and HT29), breast cancer (MCF-7and MDA-MB-213), melanoma (SK-MEK-5 and SK-MEL-2), cervical cancer (HeLa and Ca-Ski), gastric cancer (AGS and KATOIII), renal cancer (ACHN and A498), and leukemia cells (Molt4 and HL60) were obtained from the American Tissue Culture Collection (Manassas, VA) and cultured under the same conditions. These cancer cell lines were treated with the indicated parthenolide concentrations for 72 hours and harvested to determine the extent of apoptotic cell death. Transfection of the *Bcl-X_L* gene into the SCK cells was done using an expression plasmid vector encoding either human *Bcl-X_L* cDNA (a kind gift from Prof. Yuan J; ref. 16) or the control pcDNA3 (Invitrogen, Carlsbad, CA). The transfections were carried out using lipofectin (Invitrogen) according to the manufacturer's protocol. The sequence-verified *Bcl-X_L*-transfected and neo-transfected cells were selected in the presence of 600 μg/mL G418 for 2 to 3 weeks. Finally, individual colonies were isolated using cloning rings, expanded and assayed for the expression of the transfected gene using Western blot analysis. For the transient or stable transfection with the antisense *Bcl-X_L*, the Choi-CK cells were transfected with either pEGFPC3-Bcl-X_L (AS) containing the open reading frame of *Bcl-X_L* in the *Eco*RI site in the antisense orientation, or the control vector pEGFPC3 (Clontech, Palo Alto, CA). The apoptotic cells were quantified by gating the sub-G_1 fraction of the green fluorescence protein (GFP)–positive cells in the DNA histogram using the LYSIS II program. The percentage of viable cells was determined by trypan blue dye exclusion and the proportion of apoptotic cells were evaluated by Hoechst 33258 staining (1 μg/mL), which is a DNA-binding dye. At least 400 cells were counted at each time point and all the counting was carried out in a blinded manner.

Detection of DNA fragmentation. The cholangiocarcinoma cells (1×10^6) were seeded in 6 cm Petri dishes and allowed to attach. The cells were treated with the indicated parthenolide concentrations for 72 hours. In order to analyze the genomic DNA, the cells were harvested and collected together with the nonattached cells in the supernatant. The cells were resuspended in 0.5 mL of a lysis buffer [50 mmol/L Tris-HCl, 100 mmol/L EDTA, 0.5% SDS (pH 8.0)] containing 0.1 mg/mL RNase A. The DNA was extracted and separated on 1.5% agarose gels and electrophoresed in the presence of 0.5 μg/mL ethidium bromide, as described previously (15).

Flow cytometric analysis. The cholangiocarcinoma and the other cancer cells (1×10^6) were collected at set time intervals for flow cytometry using a FACScan or FACSCalibur (Becton Dickinson, San Jose, CA) with an argon laser at a wavelength of 488 nm. The trypsinized monolayer cells and the detached cells were collected at set intervals after the parthenolide treatment. Propidium iodide (40 μg/100 μL PBS) was added to 1×10^6 cells suspended in 800 μL PBS together with 100 μL RNase A (1 μg/mL), and the mixture was incubated at 37°C for 30 minutes prior to the flow cytometric analysis of 2×10^4 cells, as described elsewhere (17). The cell cycle was analyzed using ModFit LT 3.0 software program (Verity Software House, Topsham, ME). The sub-G_1 fraction was estimated by gating the hypodiploid cells in the DNA histogram using the LYSIS II program.

Fas and FasL mRNA expression. In order to prepare the single-stranded cDNA, the mRNA was reverse-transcribed with the oligo d(T)15 primers (Amersham Pharmacia Biotech, Piscataway, NJ), which was followed by PCR amplification of the *Fas* mRNA or *FasL* mRNA. Amplification was carried out for 30 cycles in a thermal cycler (Applied Biosystems, Foster City, CA), for *β-actin* as an internal control and *Fas*. Each cycle consisted of 1 minute of denaturation at 94°C, 1 minute of annealing at 57°C, and 1 minute of extension at 72°C. The sequences used were as follows: *Fas* (forward, 5′-CGGAGGATTGCTAACAAC-3′; reverse, 5′-TTGGTATTCTGGGTCCG-3′; ref. 18) and *β-actin* (forward, 5′-CGTTCTGGCGGCACCACCAT-3′; reverse, 5′-GCAACTAAGTCATAGTCCGC-3′; ref. 19). The *FasL* reverse transcriptase-PCR amplification was obtained for 35 cycles. The *FasL* primer sequences are as follows: forward, 5′-CAAGTCCAACTCAAGGTCCAT-3′ (nucleotides 641-661); reverse, 5′-AACGTATCTGAGCTCTCTCTG-3′ (nucleotides 681-710; ref. 20). The PCR conditions consisted of 1 minute of denaturation at 94°C, 1 minute of annealing at 55°C, and 1 minute of extension at 72°C. The PCR products were analyzed by electrophoresis on 1.2% agarose gels.

Cell lysis and immunoblotting. The cells were lysed and the nuclei were collected by centrifugation through a 30% sucrose solution (800 × *g*, 10 minutes at 4°C), the mitochondria were collected at 10,000 × *g* for 20 minutes at 4°C, and the remaining cell membranes were removed by centrifugation at 100,000 × *g* for 45 minutes at 4°C, as described elsewhere (17). The mouse monoclonal antibodies against p53 (DO-1) and Bcl-X_L (H-5), rabbit polyclonal antibody against Bak (G-23), Bad (K-17), Bax (N-20), and Hsp60 (H-1), and goat polyclonal antibody against Bid (C-20) and actin (C-11), were acquired from Santa Cruz (Santa Cruz, CA). The mouse monoclonal antibody against Bcl-2 (Ab-1) was obtained from Calbiochem (San Diego, CA). The mouse monoclonal antibodies against poly(ADP-ribose)polymerase (C2-10) and against cytochrome *c* (6H2.B4) were purchased from BD-PharMingen (San Diego, CA).

Measurement of the reactive oxygen species and mitochondrial transmembrane potential ($\Delta\Psi$m). The intracellular generation of reactive oxygen species (ROS) was measured using the oxidation-sensitive fluorescein 5,6-carboxy-2′,7′-dichlorofluorescein diacetate (Molecular Probes, Eugene, OR) as described elsewhere (21). The fluorescence of 2′,7′-dichlorofluorescein, which is the highly oxidized form of 5,6-carboxy-2′,7′-dichlorofluorescein, was measured using laser scanning confocal microscopy (Zeiss LSM510). In order to measure the $\Delta\Psi_m$, the cells were treated with 10 μmol/L parthenolide for the indicated time. 5,5′,6,6′-Tetraethylbenzimidazocarbocyanine iodide (5 μg/mL, JC-1; Molecular Probes) was then added to the medium, and incubation was continued for 15 minutes in the dark. The stained cells were harvested, washed once in PBS and analyzed by flow cytometry, as described elsewhere (15). At a relatively high $\Delta\Psi_m$, the dye JC-1 forms J-aggregates, which emit at 590 nm (FL-2 channel). However, in the absence of or at a low $\Delta\Psi_m$, JC-1 exists as a monomer, remaining in the cell but emitting at 527 nm (FL-1 channel).

Immunofluorescence. The cells were grown on glass coverslips, fixed with 4% paraformaldehyde, permeabilized in PBS containing 0.2% Triton X-100, and blocked with 1% bovine serum albumin. The transient transfection of Bax in fusion with the GFP gene into the SCK cells was done using lipofectin (Invitrogen) according to the manufacturer's protocol. The cells were incubated overnight with a rabbit polyclonal antibody to Bax (N-20) at 4°C, washed, and incubated with tetramethylrhodamine isothiocyanate isomer R–conjugated swine anti-rabbit immunoglobulin. After the final wash, the cells were stained with 1 μg/mL Hoechst 33258 for 15 minutes to visualize the nuclei, and mounted with 50% glycerol in PBS at 4°C. The cells were examined using laser scanning microscopy (LCM 510, Carl Zeiss, Jena, Germany).

Quantification. The densitometric data was analyzed using a Personal Densitometer SI (Molecular Dynamics, Sunnyvale, CA). The expression levels of each gene relative to the vehicle-treated control were calculated by normalizing the results against the level of glyceraldehyde-3-phosphate dehydrogenase mRNA or actin protein, and calculating the ratio of the mRNAs from the treated cells for the indicated time intervals with the untreated cells.

Statistical analysis. The data is presented as a mean ± SE of at least three independent experiments done in duplicate. Representative blots are shown. All the data was entered into the Microsoft Excel 5.0, and GraphPad Software was used to perform the two-tailed *t* tests or the analysis of the variance, where appropriate. *P* values < 0.05 were considered significant.

Results

Detection and quantification of parthenolide-induced apoptosis. The survival of the cholangiocarcinoma cells following treatment with various parthenolide concentrations was measured. Parthenolide effectively triggered cell death in a dose-dependent manner within 72 hours (Fig. 1*A*). Treatment with 10 μmol/L parthenolide for 72 hours induced cell death in 49.5 ± 2.9% (mean ± SE) of the SCK cells, 35.2 ± 3.8% of the JCK cells, 30.3 ± 2.4% of the Cho-CK cells, and 35.5% ± 3.3% of the Choi-CK cells. Apoptotic cell death of the SCK cells was significantly more pronounced than that of the other cell lines ($P < 0.05$). Therefore, this parthenolide concentration was used in the subsequent experiments. The cells treated with 10 μmol/L parthenolide were stained with Hoechst

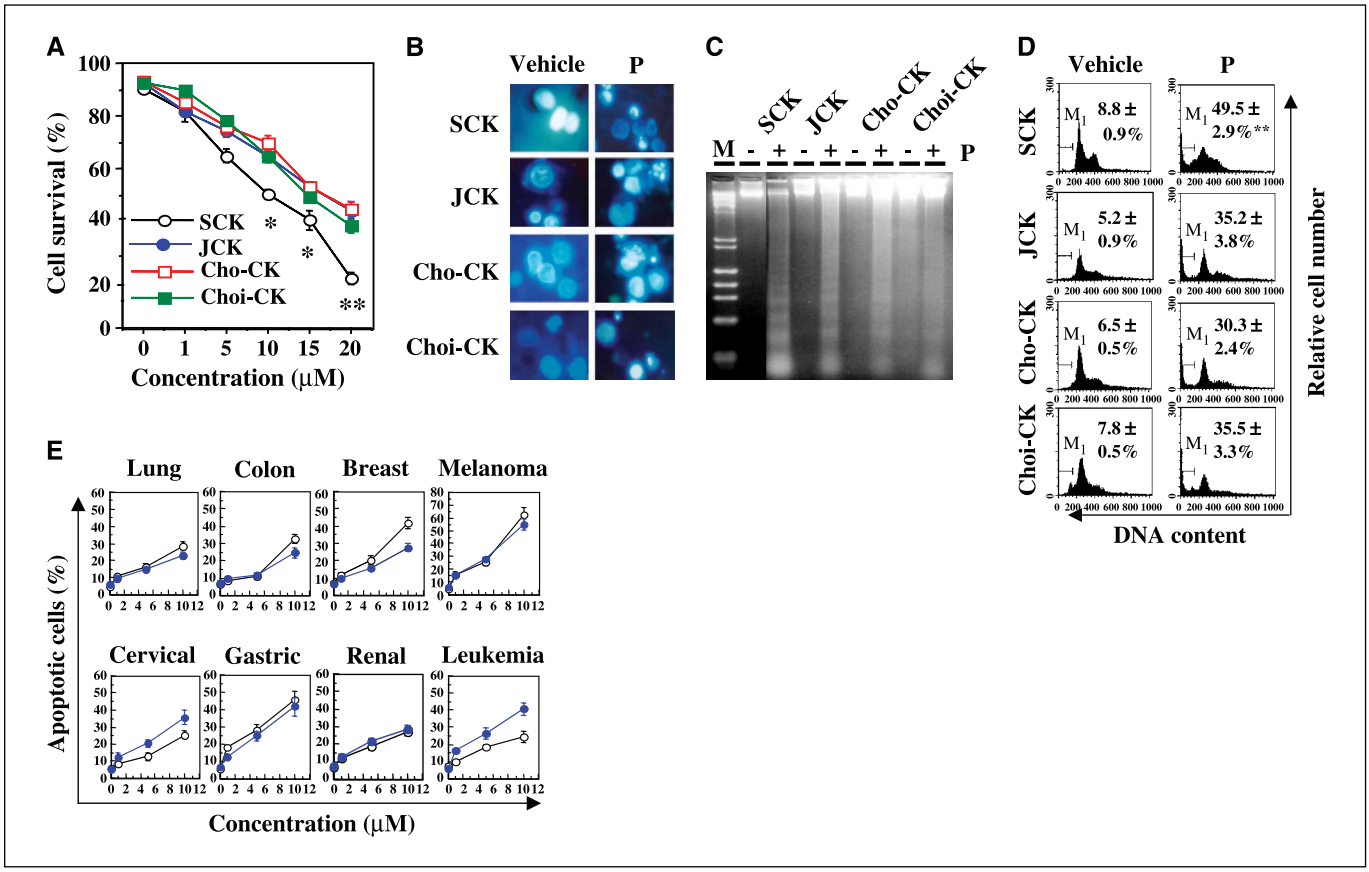

Figure 1. Kinetics of apoptosis following drug treatment. *A,* the cells were treated continuously with various parthenolide concentrations for 72 hours. The SCK, JCK, Cho-CK, and Choi-CK cells were harvested and the number of viable cells were counted by trypan blue dye exclusion. At least 400 cells were counted and all the counting was carried out in a blinded manner. *Points,* mean; *bars,* ±SE. *, $P < 0.05$; **, $P < 0.01$ compared with each mean value of JCK, Cho-CK, or Choi-CK cells. *B,* the cells were treated continuously with 10 μmol/L parthenolide (P) or the vehicle for 72 hours and were then stained with Hoechst 33258. The fraction of apoptotic cells was determined using fluorescence microscopy. *C,* induction of internucleosomal DNA fragmentation by parthenolide (P). The cells were treated with 10 μmol/L parthenolide or the vehicle (−) for 72 hours, the DNA was extracted and analyzed by agarose gel electrophoresis in the presence of ethidium bromide. The experiments were done at least thrice and the result of one representative experiment is shown. Lane M, molecular weight markers. *D,* quantification of the apoptotic fraction by flow cytometric analysis in SCK, JCK, Cho-CK, or Choi-CK cells treated with 10 μmol/L parthenolide (P) or the vehicle for 72 hours. The sub-G_1 fraction was estimated by gating the hypodiploid cells in the histogram using the LYSIS II program. The DNA content is plotted on the linear abscissa (M_1, apoptotic fraction). *Points,* mean; *bars,* ±SE. **, $P < 0.01$, compared with the cells treated with parthenolide. *E,* effects of parthenolide on the apoptotic cell death in the various human cancer cells including lung cancer cells A549 (○) and NCIH522 (●), colon cancer cells HCT116 (○) and HT29 (●), breast cancer cells MCF-7 (○), and MDA-MB-213 (●), melanoma cells SK-MEK-5 (○) and SK-MEL-2 (●), cervical cancer cells, HeLa (○) and Ca-Ski (●), gastric cancer cells AGS (○) and KATOIII (●), renal cancer cells ACHN (○) and A498 (●), and leukemia cells Molt4 (○) and HL60 (●). Quantification of the apoptotic fraction by flow cytometric analysis in the cells treated with 0, 1, 5, or 10 μmol/L of parthenolide (P) for 72 hours. The sub-G_1 fraction was estimated by gating the hypodiploid cells in the histogram using the LYSIS II program. *Points,* mean; *bars,* ±SE.

33258 (1 μg/mL) to measure the level of apoptotic cell death, which was revealed by the condensed chromatin and fragmented nuclear morphologies in all four cell lines (Fig. 1*B*). The cells displayed disintegrated nuclei and nonrandom DNA fragmentation, as assessed by agarose gel electrophoresis of the genomic DNA (Fig. 1*C*). The SCK cells showed a higher proportion of apoptotic internucleosomal DNA fragmentation than the other cell lines. In addition, the apoptotic cell death was further confirmed using flow cytometric analysis. Parthenolide effectively induced a substantial apoptotic sub-G_1 fraction in all the cholangiocarcinoma cell lines compared with the vehicle (Fig. 1*D*). Furthermore, the apoptotic fraction of the SCK cells was significantly higher in the SCK cells than in the other cell lines (49.5% versus 35.2%, 30.3%, or 35.5%; $P < 0.01$). These results are consistent with the increased apoptosis of SCK cells.

In order to determine the effect of the parthenolide on other human cancer cell lines indicated, they were treated with 0, 1, 5, or 10 μmol/L parthenolide for 72 hours. Parthenolide effectively induced apoptosis in the various human cancer cell lines in a range of 22.7% to 62% 72 hours after treatment. In particular, melanoma cells, SK-MEK-5, and SK-MEL-2 showed a higher susceptibility to parthenolide-induced apoptosis than the other cancer cells, i.e., the proportion of apoptotic cells were 62% and 54.5%, respectively. In contrast, lung cancer cells, A549 and NCIH522 showed minimal susceptibility, i.e., 32.5% and 22.7%, respectively (Fig. 1*E*).

The effective concentration (10 μmol/L) of parthenolide seems to be quite high. Therefore, this study examined whether or not a low parthenolide concentration also has an antitumor effect on the cholangiocarcinoma cell lines. The results showed that a sublethal dose (2 μmol/L) of parthenolide effectively inhibited cell growth by inhibiting the cell cycle progression compared with the vehicle controls. Flow cytometric analysis revealed that parthenolide significantly enhanced G_1 arrest in all four cell lines, which was accompanied by a decrease in the S phase (Table 1). These results suggest that the low parthenolide concentration can be connected to its *in vivo* antitumor effect.

Table 1. Cell cycle phase distribution in the cholangiocarcinoma cells following treatment with a sublethal dose of parthenolide

	SCK (%)		JCK (%)		Cho-CK (%)		Choi-CK (%)	
	Vehicle	Parthenolide	Vehicle	Parthenolide	Vehicle	Parthenolide	Vehicle	Parthenolide
G_1	42.7 ± 5.2	62.0 ± 6.9*	57.8 ± 4.5	74.0 ± 7.7†	52.6 ± 6.6	75.9 ± 7.3*	62.5 ± 5.8	77.4 ± 7.4†
S	51.0 ± 5.6	22.3 ± 2.9*	32.2 ± 3.4	25.5 ± 1.8†	46.6 ± 3.4	22.4 ± 1.2*	35.5 ± 5.1	20.6 ± 3.3†
G_2-M	6.2 ± 2.1	15.7 ± 1.1*	1.2 ± 0.1	3.3 ± 0.2†	1.0 ± 0.3	1.6 ± 0.2	1.8 ± 0.3	2.6 ± 0.2

NOTE: Cell cycle phase distribution was determined by flow cytometric analysis following treatment with 2 μmol/L parthenolide for 72 hours. The values are means ± SE.
*$P < 0.01$.
†$P < 0.05$.

Expression of p53 and Bcl2/Bcl-X_L. In order to examine the genetic changes that might be related to the drug susceptibility, the expression of the p53 and Bcl-2/Bcl-X_L proteins was examined. This study used a mouse monoclonal antibody (DO-1), which recognizes the wild-type and mutant p53 proteins of human origin. The SCK cells did not express the p53 protein. The other three ordinary cholangiocarcinoma cell lines expressed either the wild-type or the mutant p53 (Fig. 2*A*). The *p53* gene is one of the most frequently mutated genes in all types of cancer (22), with most mutations occurring in exons 5 to 8 (23). Mutations occurring in those regions are usually missense mutations that alter the DNA binding site conformation. Single-strand conformation polymorphism analysis of the genetic changes revealed that the Choi-CK cells did not have any shifted bands in the *p53* gene in exons 5 to 8. In contrast, abnormal band shifts were detected in exon 6 of the JCK cells and exon 8 of the Cho-CK cells, suggesting a dysfunction in the *p53* gene in the JCK and Cho-CK cells but a wild-type p53 function in the Choi-CK cells (data not shown).

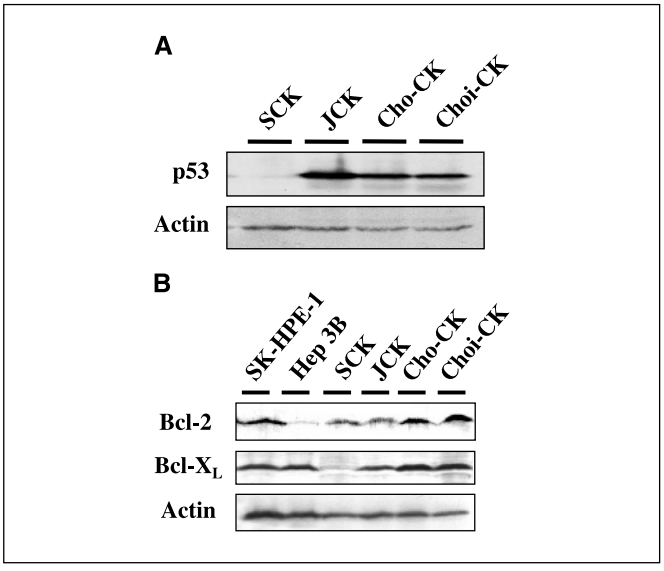

Figure 2. The expression of the p53 protein and the Bcl2/Bcl-X_L protein in the cholangiocarcinoma cell lines. *A,* 30 μg of the extracted proteins were resolved by 12% SDS-PAGE and transferred to the membrane. The blots were probed with a monoclonal antibody to p53 (DO-1). The blots were then stripped and reprobed with a monoclonal antibody to actin as the loading control. The experiments were done at least thrice, and the result of one representative experiment is shown. *B,* immunodetection of Bcl-2 or Bcl-X_L was done using a mouse anti-Bcl-2 monoclonal antibody (Ab-1) or a mouse anti-Bcl-X_L monoclonal antibody (H-5). The blots were then stripped and reprobed with a monoclonal antibody to actin as the loading control.

Bcl-2 protects the cells against apoptosis, and the inhibition of Bcl-2 expression promotes apoptosis in response to a variety of stimuli (24, 25). Therefore, the Bcl-2 protein expression level was determined in the cholangiocarcinoma cell lines. All the cholangiocarcinoma cell lines exhibited Bcl-2 expression. However, the expression of Bcl-X_L, which is another Bcl-2-related anti-apoptotic protein, was negative in the SCK cells, whereas it was positive in the other three adenomatous cholangiocarcinoma cells (Fig. 2*B*). Human hepatoma cells, SK-HEP-1 and Hep 3B cells were used as the positive and negative controls of Bcl-2 expression, respectively (17).

Modulation of p53, Fas/FasL, and Bcl2/Bcl-X_L expression by parthenolide. Western blot analysis was done after treating the cholangiocarcinoma cell lines with 10 μmol/L parthenolide for 72 hours. Parthenolide significantly increased the p53 protein expression level in the adenomatous cholangiocarcinoma cells irrespective of the p53 function (Fig. 3*A*).

The expression of *Fas/FasL* in cholangiocarcinoma cells was then examined because Fas/FasL mediates various types of drug-induced apoptosis (26). Parthenolide decreased the *Fas* mRNA expression level in all the cholangiocarcinoma cell lines. Parthenolide also decreased the *FasL* mRNA expression level in the three adenomatous cholangiocarcinoma cell lines but not in the sarcomatous SCK cells (Fig. 3*B*). These observations are consistent with a report showing that parthenolide suppresses the *Fas/FasL* expression at the mRNA level in T cells (27). However, parthenolide did not inhibit *FasL* expression in the susceptible SCK cells. Although the mechanism of this different regulation of *FasL* is unclear, the drug-induced *FasL* transcription and apoptosis was reported to be inhibited by Bcl-X_L (28). Therefore, *FasL* expression may not be inhibited by parthenolide in the Bcl-X_L-defective SCK cells. This study used human hepatoma cells, SK-HEP-1 and Hep 3B cells, as positive and negative controls, respectively. The SK-HEP-1 cells expressed *Fas* mRNA and the Hep 3B cells did not express *Fas* mRNA, as described elsewhere (17).

In order to examine the potential role of the Bcl-2 family members in the parthenolide-induced apoptosis, this study examined the effects of parthenolide on the expression or cleavage of several members of this family. Parthenolide did not alter the expression of the antiapoptotic Bcl-2 or Bcl-X_L in the adenomatous cholangiocarcinoma cell lines after being treated with 10 and even

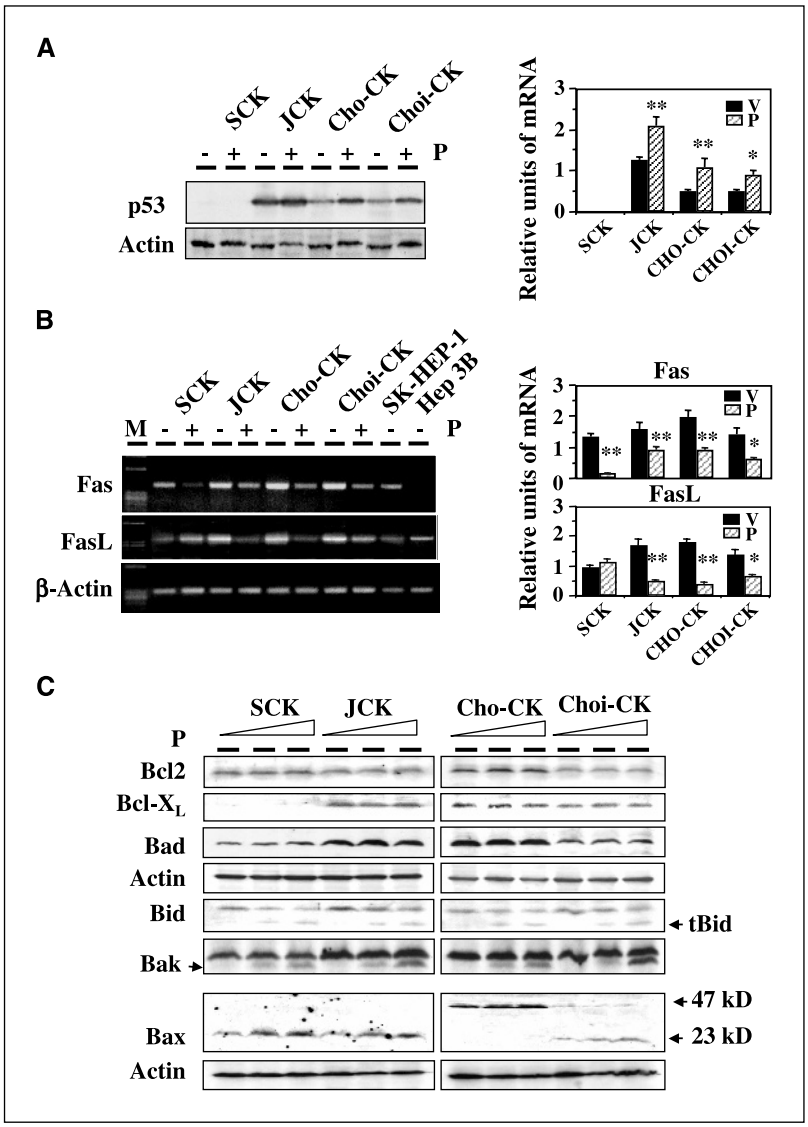

Figure 3. Modulation of p53, *Fas/FasL*, and Bcl-2 family expression by parthenolide. *A,* immunoblotting of p53 in the cholangiocarcinoma cells cultured in the presence (+) of 10 μmol/L parthenolide (P) or vehicle (−; V) for 72 hours. Thirty micrograms of the extracted proteins were resolved by 12% SDS-PAGE and transferred to the membrane. The blots were probed with a monoclonal antibody to p53 (DO-1) and then stripped and reprobed with a monoclonal antibody to actin as the loading control. The experiments were done at least thrice and the result of one representative experiment is shown. *Columns,* means; *bars,* ± SE. *, $P < 0.05$; **, $P < 0.01$. *B,Fas/FasL* mRNA expression was analyzed by reverse transcriptase-PCR using the primers for *Fas/FasL* in the cholangiocarcinoma cells cultured in the presence (+) of 10 μmol/L parthenolide (P) or vehicle (−; V) for 72 hours. The experiments were done at least thrice and the result of one representative experiment is shown. *Columns,* means; *bars,* ± SE. *, $P < 0.05$; **, $P < 0.01$. *C,* immunoblotting of Bcl-2, Bcl-X_L, Bad, Bid, Bak, and Bax in the cholangiocarcinoma cells cultured in increasing concentrations, 0 μmol/L (first lane), 10 μmol/L (second lane), and 20 μmol/L (third lane), of parthenolide (P) for 72 hours. Thirty micrograms of the extracted proteins were resolved by 12% SDS-PAGE and transferred to the membrane. The blots were probed with a monoclonal or polyclonal antibody against Bcl-2 (Ab-1), Bcl-X_L (H-5), Bad (K-17), Bid (C-20), Bak (G-23), and Bax (N-20), and then stripped and reprobed with the monoclonal antibody to actin as a loading control. The experiments were done at least thrice and the result of one representative experiment is shown.

20 μmol/L parthenolide for 72 hours (Fig. 3*C*). However, considering that the SCK cells exhibited defective Bcl-X_L expression and altered *FasL* regulation, the defective Bcl-X_L expression might have contributed to the susceptibility to parthenolide-induced apoptosis. This is because the parthenolide-mediated anticancer effects may be related to oxidative stress, as described in the literature (15). Accordingly, the involvement of the proapoptotic Bcl-2 family, such as Bid, Bad, Bak, and Bax, was examined. In contrast to there being no alterations in Bad expression, cleavages of Bid by parthenolide were shown in the four cholangiocarcinoma cell lines. Parthenolide concomitantly induced Bak and Bax expressions in all four cell lines, even though the Cho-CK cells might express the high molecular weight oligomer or complex of Bax, which is consistent with a previous report (29). The caspase-8 cleavage of Bid generates tBid, which is inserted into the mitochondrial outer membrane. The mitochondrial tBid subsequently recruits Bax into the outer membrane bilayer and induces the intramembrane oligomerization of Bax (30) and Bak (31), causing these proapoptotic Bcl-2 members to form the proposed conduit for the release of cytochrome *c* from the organelles (32).

Ectopic overexpression of Bcl-X_L leads to resistance to parthenolide-mediated apoptosis. Two stable cell lines that overexpress Bcl-X_L from the Bcl-X_L defective SCK cells, termed XL-21 and XL-26, were established in order to determine if Bcl-X_L expression contributes to resistance against parthenolide-induced apoptosis. The vehicle did not alter the level of apoptotic cell death in both the vector control cells and Bcl-X_L transfectants. In contrast, Bcl-X_L expression significantly inhibited the parthenolide-induced apoptosis the stable transfectants to ~50% of the level of the control cells in (29.2 ± 3.8% and 33.4 ± 2.6% versus 74.5 ± 4.2% and 64.5 ± 6.6%; $P < 0.01$; Fig. 4*A*). Therefore, Bcl-X_L expression reduced the sensitivity to drug-induced apoptosis, which might be mediated by the inhibition of oxidative damage. In order to test this hypothesis, another apoptosis inducing agent, 4-(*N*-hydroxyphenyl)retinamide (4HPR), was used because this drug has also been reported to induce oxidative injury in cancer cells (33). Bcl-X_L expression also effectively inhibited the 4HPR-induced apoptosis to ~40% of the control cells (37.2 ± 4.8% and 35.5 ± 5.4% versus 94.2 ±6.5% and 84.4 ± 7.5%; $P < 0.01$) in the stable transfectants (Fig. 4*B*).

Two stable cell lines (AS1 and AS2) transfected with an antisense expression plasmid of *Bcl-X_L* in fusion with a GFP were established

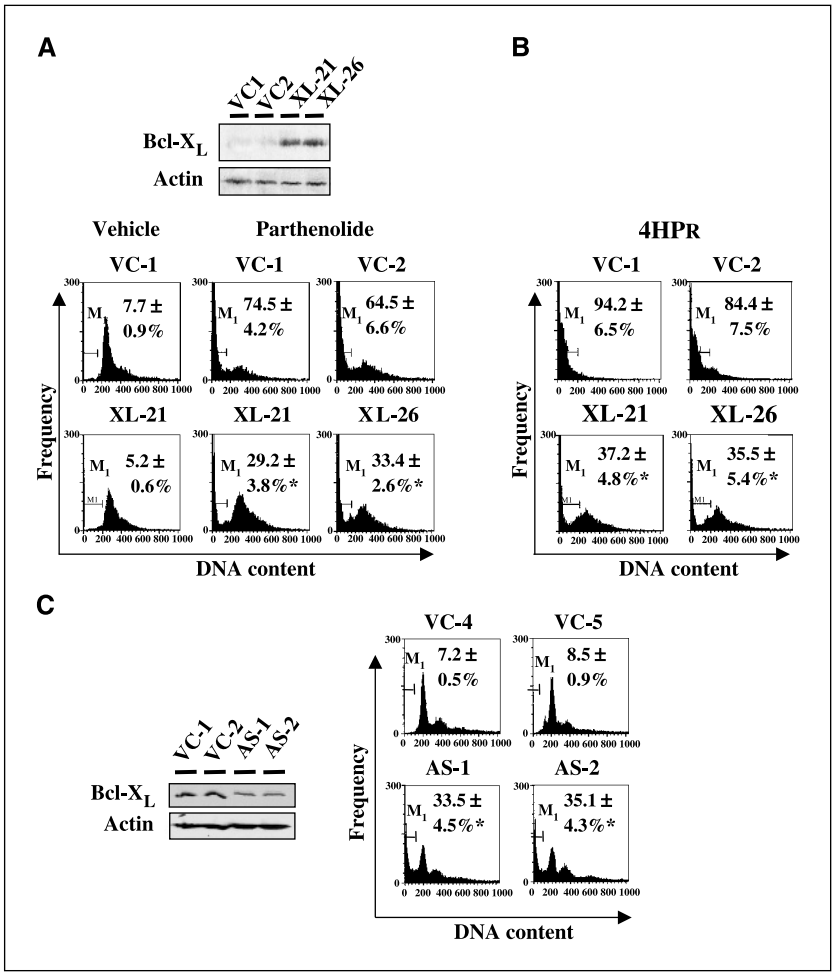

Figure 4. Effect of Bcl-X_L expression on apoptotic cell death in SCK cells. *A,* protein expression of Bcl-X_L in the stably transfected SCK cells (XL-21 and XL-26) compared with the vector control cells (VC-1 and VC-2). Immunodetection of Bcl-X_L was done using the mouse anti-Bcl-X_L monoclonal antibody (H-5). The blots were then stripped and reprobed with the monoclonal antibody to actin as a loading control (*top*). Quantification of the apoptotic fraction was done by flow cytometric analysis. The cells were grown for 72 hours in the presence of either the vehicle or 10 μmol/L parthenolide. The sub-G_1 fraction was estimated by gating the hypodiploid cells in the histogram using the LYSIS II program. The DNA contents are plotted on the linear abscissa (M_1, apoptotic fraction). *Points,* mean; *bars,* ± SE. *, $P < 0.01$ compared with the vector controls. *B,* the cells were grown for 72 hours in the presence of the vehicle or 10 μmol/L 4HPR. The sub-G_1 fraction was estimated by gating the hypodiploid cells in the histogram using the LYSIS II program. The DNA contents are plotted on the linear abscissa (M_1, apoptotic fraction). *Points,* mean; *bars,* ± SE. *, $P < 0.01$ compared with the vector controls. *C,* protein expression of Bcl-X_L in the stably transfected Choi-CK cells (AS1 and AS2) with antisense expression plasmid of *Bcl-X_L* in fusion with a GFP compared with the vector control cells (VC-4 and VC-5; left). The stable transfectants were then treated with either 10 μmol/L parthenolide or the vehicle for 36 hours. The cells were harvested and stained with propidium iodide. Quantification of the apoptotic fraction was done by flow cytometric analysis (right). *, $P < 0.01$ compared with the vector controls.

to determine if the prevention of Bcl-X_L expression might lead to the enhanced susceptibility to parthenolide in Bcl-X_L-positive Choi-CK cells. The Bcl-X_L expression was effectively inhibited by >65% in those transfectants. The AS1 and AS2 cells were more susceptible to parthenolide, i.e., ~33.5% and 35.5% of the transfectants were apoptotic ($P < 0.01$), compared with 7.2% and 8.5% of the empty vector control cells (VC-4 and VC-5; Fig. 4*C*). Similarly, the transient transfection experiments showed that the Choi-CK cells transfected with the antisense *Bcl-X_L* cDNA were more susceptible to parthenolide, i.e., ~71.9% of the transfectants were apoptotic ($P < 0.01$), compared with 40.3% of the empty vector control cells (data not shown). These results suggest that the inhibition of Bcl-X_L expression correlates positively with the apoptotic cell death in Choi-CK cells.

Bcl-X_L overexpression inhibits mitochondrial translocation of Bax and the generation of reactive oxygen species. Because Bid activation and Bak and Bax overexpression did not seem to differentiate the drug susceptibility according to the Bcl-X_L expression level, this study determined if Bcl-X_L expression regulates the mitochondrial translocation of Bax between the Bcl-X_L-positive (XL-21 and XL-26) and Bcl-X_L-negative cells (VC-1 and VC-2). Following a death signal, Bax translocates from the cytosol to the mitochondria at which time the Bax conformation changes (34). This mitochondrial localization and its oligomerization play an important role in triggering apoptosis (35). Bak, which is another proapoptotic molecule, normally resides in the mitochondria and undergoes a rearrangement to form the homo-oligomeric complexes following Bax insertion into the mitochondria. Despite this functional cooperation between Bax and Bak, Bax is essential for mitochondrial permeabilization (36). Therefore, the Bax expression level was measured in the cytosol and in the mitochondrial extracts after drug treatment for 48 hours (Fig. 5*A*). Parthenolide effectively decreased the cytosolic Bax level in the vector control cells (VC-1 and VC-2), whereas it had little effect on the Bcl-X_L transfectants (XL-21 and XL-26). Accordingly, the accumulation of Bax increased proportionally in the mitochondria of the vector control cells. In order to further confirm the inhibition of Bax translocation by Bcl-X_L, the SCK cells were transiently cotransfected with the GFP-Bax fusion vector and a mitochondria targeting vector pDsRed1-Mito (Clontech), and then treated with parthenolide (Fig. 5*B*). Bax was localized in the cell cytoplasm and nucleus. Parthenolide effectively translocated the Bax to the perinuclear area, which overlaps with the localization of the mitochondria targeting the fluorescence. In contrast, parthenolide barely translocated Bax to the mitochondria in the SCK cells transfected with Bcl-X_L, which is localized at the mitochondria. This suggests that Bcl-X_L effectively inhibited the parthenolide-induced translocation of cytosolic Bax to the mitochondria. Previously, it was reported that parthenolide induced oxidative damage in hepatoma cells in a glutathione-sensitive manner and that this oxidative damage led to ROS generation, $\Delta\Psi_m$ reduction, cytochrome *c* release, caspase activation, and finally apoptotic cell

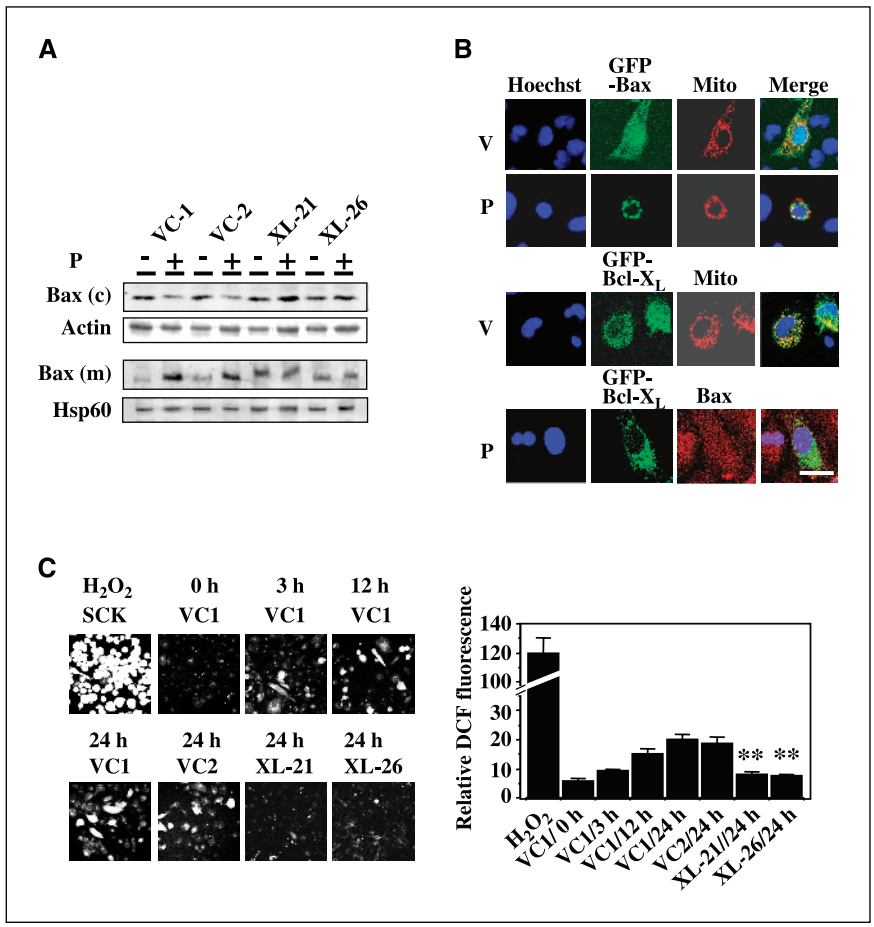

Figure 5. Reduction of ROS generation by ectopic overexpression of Bcl-X_L in SCK cells. *A,* the cells were treated with 10 μmol/L parthenolide (P) for 48 hours. Thirty micrograms of cytosolic (c) and mitochondrial (m) proteins were separated by 15% SDS-PAGE. Immunodetection of Bax was done using specific antibodies, as detailed in Materials and Methods, and was visualized by enhanced chemiluminescence. The actin and Hsp60 antibodies were used as the cytoplasmic and mitochondrial markers, respectively. The experiments were done at least thrice and the result of one representative experiment is shown. *B,* the cells cotransfected with the GFP-Bax fusion vector and a mitochondrial targeting pDsRed-Mito (*top*) or with the GFP-Bcl-X_L fusion vector and the mitochondrial targeting pDsRed-Mito (*middle*), or transfected with the GFP-Bcl-X_L fusion vector only (*bottom*) were for 1 μg/mL Hoechst 33258 staining in order to visualize the nuclei (blue) and for indirect immunofluorescence staining for Bax (red). The cells were incubated in the presence of 10 μmol/L parthenolide (P) or vehicle (V) for 48 hours. The experiments were done at least thrice and the result of one representative experiment is shown. *Bar,* 20 μm. *C,* following treatment with 10 μmol/L parthenolide, 2′,7′-dichlorofluorescein fluorescence was measured using confocal microscopy at the indicated time intervals in the control cells transfected with the empty vector. 2′,7′-Dichlorofluorescein fluorescence of the SCK cells stably expressing Bcl-X_L was compared with that of the control cells after treating them with 10 μmol/L parthenolide for 24 hours. The relative 2′,7′-dichlorofluorescein (*DCF*) fluorescence intensity per cell was calculated as described in Materials and Methods (right). *Columns,* means; *bars,* ± SE. **, $P < 0.01$ compared with the vector controls treated with parthenolide for 12 hours. The experiments were done at least thrice and the result of one representative experiment is shown.

death (15). In order to investigate the mechanism whereby Bcl-X_L inhibited the parthenolide-induced apoptosis downstream of Bax translocation, ROS generation was measured in the cells stably expressing Bcl-X_L and compared them with the ROS level in the control cells transfected with the empty vector because this protein is a well-known antiapoptotic protein that functions during oxidative damage (37). ROS generation was increased in the vector control cells in a time-dependent manner. The maximum 2′,7′-dichlorofluorescein fluorescence intensity was reached within 24 hours of the parthenolide treatment (Fig. 5*C*). The ectopic expression of Bcl-X_L effectively decreased the production of ROS to 40% of the level in the control cells. H_2O_2 was used as a positive control.

Bcl-X_L overexpression inhibits $\Delta\Psi_m$ reduction, cytochrome *c* release, and poly(ADP-ribose) polymerase cleavage. ROS generation is believed to mediate $\Delta\Psi_m$ reduction, which in turn causes the release of cytochrome *c* and initiates the apoptotic cascade. Therefore, this study investigated whether or not the ectopic expression of BCL-X_L modulates this initiation of the mitochondrial/intrinsic cascade of apoptosis. The expression of Bcl-X_L inhibited the parthenolide-induced $\Delta\Psi_m$ reduction in the stable XL-26 transfectants, compared with the vector control VC-2 cells (6 ± 0.6% versus 27.5 ± 4%; $P < 0.01$). Similar results were obtained using XL-21 cells, compared with the VC-1 cells (8 ± 01% versus 25.5 ± 3.5%; $P < 0.01$; data not shown). Another oxidative stress inducing agent, 4HPR, was used to further examine this phenomenon. Compared with the VC-1 cells, Bcl-X_L expression also effectively inhibited 4HPR-induced apoptosis to ~42% of the level of the control cells (25 ± 3% versus 60 ± 5%; $P < 0.01$) in the stable XL-26 transfectants (Fig. 6*A*), and to ~35% (30 ± 3% versus 65 ± 5%; $P < 0.01$) in the XL-21 cells (data not shown). Furthermore, Bcl-X_L decreased the release of cytochrome *c* in the cytoplasmic fraction and poly(ADP-ribose) polymerase cleavage (Fig. 6*B*). Therefore, Bcl-X_L inhibits ROS generation, subsequent $\Delta\Psi_m$ reduction, cytochrome *c* release, and poly(ADP-ribose) polymerase cleavage. This suggests that Bcl-X_L effectively inhibits the oxidative damage induced by parthenolide and in turn decreases the susceptibility of the cells to apoptotic cell death.

Discussion

DNA ladder, Hoechst staining, and flow cytometric analysis was used to confirm the parthenolide-induced apoptosis in cholangiocarcinoma cells as well as in other various cancer cells examined in this study. In particular, parthenolide-mediated apoptotic cell death was observed in all four cell lines (designated as SCK, JCK, Cho-CK and Choi-CK cells), but the SCK cells were more susceptible (Fig. 1*A*) whereas a sublethal dose of parthenolide (2 μmol/L) inhibited tumor cell growth via G_1 arrest in all four cell lines. In order to discriminate the genetic heterogeneity involved in the different parthenolide susceptibility, the basal expression of p53 and Bcl-2/Bcl-X_L was compared. The more susceptible SCK cells showed defective p53 and Bcl-X_L expression, compared with the other adenomatous cholangiocarcinoma cells.

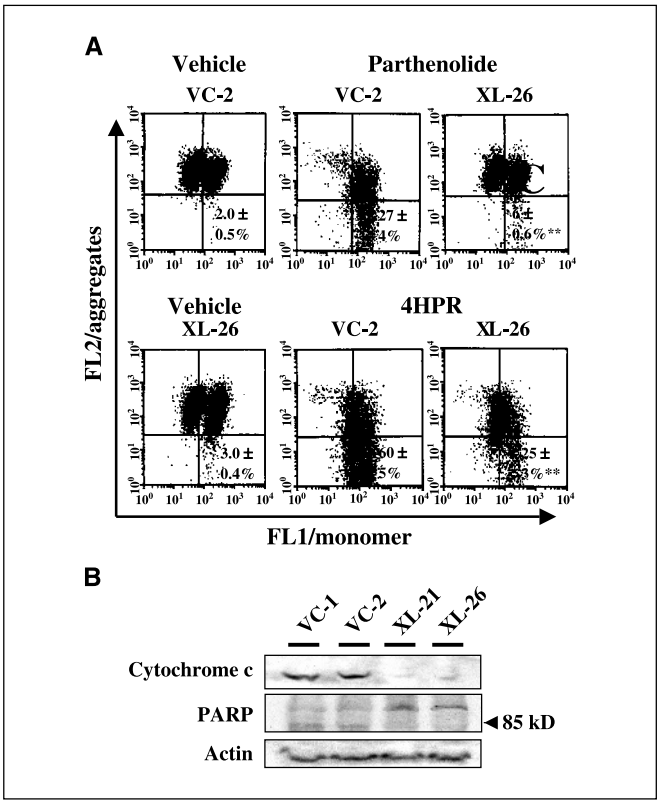

Figure 6. Inhibition of $\Delta\Psi_m$ reduction, reduction, cytochrome *c* release, and Bax translocation by ectopic overexpression of Bcl-X_L in SCK cells. *A,* the SCK cells stably expressing Bcl-X_L were treated with 10 μmol/L parthenolide or 10 μmol/L 4HPR for 72 hours and $\Delta\Psi_m$ was detected by flow cytometric analysis using the J aggregate-forming dye JC-1. Bottom right quadrant, relative intensity of the green versus red fluorescence was plotted, which revealed the range of lower fluorescence representing the loss of $\Delta\Psi_m$. This experiment was repeated thrice with similar results. Each value represents the mean ± SE of two independent experiments done in triplicate. **, $P < 0.01$ compared with the vector controls. *B,* the cells were treated with 10 μmol/L parthenolide for 72 hours. The S-100 fractions of the cytosolic proteins (30 μg) were separated by 15% SDS-PAGE. The blot was probed with the monoclonal antibody to cytochrome *c* (1:1,000) or poly(ADP-ribose) polymerase (1:2,000). Thirty micrograms of protein per lane isolated from the cell lysates were separated by 15% SDS-PAGE. The experiments were done at least thrice and the result of one representative experiment is shown.

The parthenolide induced mutant p53 overexpression in the JCK and Cho-CK cells, and the wild-type p53 overexpression in the Choi-CK cells (Fig. 3*A*). Therefore, parthenolide effectively triggered apoptotic cell death in the various types of cholangiocarcinoma cells, irrespective of whether they expressed the wild-type or mutant *p53* gene. Chemotherapeutic drugs, such as doxorubicin, methotrexate, or bleomycin, up-regulate the membrane Fas and FasL expression level, which is followed by the induction of Fas-dependent apoptosis (38–40). In this study, all four cholangiocarcinoma cell lines showed the heterogeneous expression of *Fas/FasL* mRNA. Parthenolide decreased *Fas/FasL* mRNA expression level in all the cholangiocarcinoma cells with the exception of the SCK cells where the *FasL* mRNA expression level increased. Furthermore, parthenolide also triggered apoptosis in the hepatoma cell lines, including Hep 3B and PLC/PRF cells, which are known to exhibit defective Fas expression (17). Therefore, parthenolide-induced apoptosis seems to be independent of *Fas/FasL* expression.

Parthenolide effectively induced Bax translocation to the mitochondria in the vector control cells and this translocation was minimal in the Bcl-X_L-expressing SCK cells. Even though the mechanisms responsible for Bax insertion into the mitochondrial membrane and the localization of Bax within the mitochondria are unclear, Bid, a BH3-only Bax-interacting protein, is known to trigger Bax integration in the outer mitochondrial membrane. Bid can induce a change in the Bax conformation leading to the exposure of its NH_2-terminal domain (29). The NH_2-terminal domain of Bax exerts repressing activity on the targeting of Bax to the mitochondrial membranes, possibly by interfering with the hydrophobic COOH-terminal membrane-anchoring domain (41). Bax dimerization seems to be another critical event for Bax integration in the membrane (42). Both Bcl-2 and Bcl-X_L could prevent Bax oligomerization and insertion by binding directly to Bax. Therefore, Bcl-X_L effectively prevents the Bax translocation to the mitochondria and subsequently reduces the mitochondrial membrane potential and cytochrome *c* release. The mechanism(s) by which Bax triggers the release of cytochrome *c* from the mitochondria following its membrane insertion is still unclear. However, Bax may stimulate the opening of the permeability transition pore through an interaction with the adenine nucleotide translocator (43), which may lead to channel formation (29).

Sesquiterpene lactones have an α-methylene γ-lactone functionality as an electrophilic agent and are prone to reactions with biological nucleophiles such as the sulfhydryl groups of the reduced glutathione, proteins, and parts of the DNA (44). Therefore, the decrease in the cellular glutathione levels both *in vitro* and *in vivo* has been observed in tumor cells exposed to sesquiterpene lactones (45). A previous study consistently showed that parthenolide-mediated oxidative stress resulted mainly from reduced glutathione depletion and ROS generation, and that the tumor cell sensitivity to parthenolide seems to correlate with the glutathione metabolism (15). This study showed that Bax translocation correlates with ROS production. The results showed that the Bcl-X_L-mediated inhibition of Bax translocation decreased the parthenolide-induced ROS generation upstream of oxidative stress, and subsequently inhibited the reduction in the mitochondrial membrane potential. Finally, Bcl-X_L inhibited the release of cytochrome *c* to the cytoplasm, poly(ADP-ribose) polymerase cleavage, and apoptotic cell death. These results show that Bax translocation may be critical in parthenolide-induced apoptosis and that the modulation of Bax translocation may alter the susceptibility of the cholangiocarcinoma cells to partheolide-induced apoptosis.

In summary, parthenolide and its derivatives may be effective anticancer agents against cholangiocarcinoma because they can effectively induce apoptosis in cholangiocarcinoma cells. Although the molecular mechanism(s) for the parthenolide-induced cancer cell apoptosis are poorly understood, oxidative stress and the Bcl-2 family molecules might be involved. In particular, Bid activation and Bax translocation are linked to ROS production and caspase activation. The defective expression of Bcl-X_L might increase the drug susceptibility as a result of the enhanced Bax translocation. Therefore, these molecular mechanisms may be applicable to a chemotherapeutic strategy for cholangiocarcinoma cells.

Acknowledgments

Received 11/23/2004; revised 3/13/2005; accepted 4/14/2005.

Grant support: The Korea Health 21 R&D Project, Ministry of Health and Welfare, Republic of Korea (A050328) and the 21C Frontier Functional Human Genome Project from Ministry of Science and Technology of Korea (FG04-11-01).

The costs of publication of this article were defrayed in part by the payment of page charges. This article must therefore be hereby marked *advertisement* in accordance with 18 U.S.C. Section 1734 solely to indicate this fact.

We thank Prof. Junying Yuan for providing the plasmids, and the Korea Basic Science Institute for the laser scanning microscopy.

References

1. Voravud N, Foster CS, Gilbertson JA, Sikora K, Waxman J. Oncogene expression in cholangiocarcinoma and in normal hepatic development. Hum Pathol 1989; 20:1163–8.
2. Mittal B, Deutsch M, Iwatsuki S. Primary cancers of extrahepatic biliary passages. Int J Radiat Oncol Biol Phys 1985;11:849–54.
3. Pitt HA, Nakeeb A, Abrams RA, et al. Perihilar cholangiocarcinoma. Postoperative radiotherapy does not improve survival. Ann Surg 1995;221:788–97.
4. Schoenthaler R, Castro JR, Halberg FE, Phillips TL. Definitive postoperative irradiation of bile duct carcinoma with charged particles and/or photons. Int J Radiat Oncol Biol Phys 1993;27:75–82.
5. Vauthey JN, Blumgart LH. Recent advances in the management of cholangiocarcinomas. Semin Liver Dis 1994;14:109–14.
6. Kim DG, Park SY, You KR, et al. Establishment and characterization of chromosomal aberrations in human cholangiocarcinoma cell lines by cross-species color banding. Genes Chromosomes Cancer 2001;30:48–56.
7. Johnson ES, Kadam NP, Hylands DM, Hylands PJ. Efficacy of feverfew as prophylactic treatment of migraine. Br Med J (Clin Res Ed) 1985;291:569–73.
8. Murphy JJ, Heptinstall S, Mitchell JR. Randomised double-blind placebo-controlled trial of feverfew in migraine prevention. Lancet 1988;2:189–92.
9. Hehner SP, Heinrich M, Bork PM, et al. Sesquiterpene lactones specifically inhibit activation of NF-κB by preventing the degradation of IκB-α and IκB-β. J Biol Chem 1998;273:1288–97.
10. Lyss G, Knorre A, Schmidt TJ, Pahl HL, Merfort I. The anti-inflammatory sesquiterpene lactone helenalin inhibits the transcription factor NF-κB by directly targeting p65. J Biol Chem 1998;273:33508–16.
11. Kupchan SM, Eakin MA, Thomas AM. Tumor inhibitors. 69. Structure-cytotoxicity relationships among the sesquiterpene lactones. J Med Chem 1971; 14:1147–52.
12. Woynarowski JM, Konopa J. Inhibition of DNA biosynthesis in HeLa cells by cytotoxic and antitumor sesquiterpene lactones. Mol Pharmacol 1981;19:97–102.
13. Bork PM, Schmitz ML, Kuhnt M, Escher C, Heinrich M. Sesquiterpene lactone containing Mexican Indian medicinal plants and pure sesquiterpene lactones as potent inhibitors of transcription factor NF-κB. FEBS Lett 1997;402:85–90.
14. Hwang D, Fischer NH, Jang BC, Tak H, Kim JK, Lee W. Inhibition of the expression of inducible cyclooxygenase and proinflammatory cytokines by sesquiterpene lactones in macrophages correlates with the inhibition of MAP kinases. Biochem Biophys Res Commun 1996;226: 810–8.
15. Wen J, You KR, Lee SY, Song CH, Kim DG. Oxidative stress-mediated apoptosis: The anticancer effect of the sesquiterpene lactone parthenolide. J Biol Chem 2002; 277:38954–64.
16. Li H, Zhu H, Xu CJ, Yuan J. Cleavage of BID by caspase 8 mediates the mitochondrial damage in the Fas pathway of apoptosis. Cell 1998;94:491–501.
17. You KR, Shin MN, Park RK, Lee SO, Kim DG. Activation of caspase-8 during *N*-(4-hydroxyphenyl) retinamide-induced apoptosis in Fas-defective hepatoma cells. Hepatology 2001;34:1119–27.
18. Panayiotidis P, Ganeshaguru K, Foroni L, Hoffbrand AV. Expression and function of the FAS antigen in B chronic lymphocytic leukemia and hairy cell leukemia. Leukemia 1995;9:1227–32.
19. Wong H, Anderson WD, Cheng T, Riabowol KT. Monitoring mRNA expression by polymerase chain reaction: the "primer-dropping" method. Anal Biochem 1994;223:251–8.
20. Mita E, Hayashi N, Iio S, et al. Role of Fas ligand in apoptosis induced by hepatitis C virus infection. Biochem Biophys Res Commun 1994;204:468–74.
21. Kim H, Lee TH, Park ES, et al. Role of peroxiredoxins in regulating intracellular hydrogen peroxide and hydrogen peroxide-induced apoptosis in thyroid cells. J Biol Chem 2000;275:18266–70.
22. Levine AJ. The p53 tumor-suppressor gene. N Engl J Med 1992;326:1350–2.
23. Nigro JM, Baker SJ, Preisinger AC, et al. Mutations in the p53 gene occur in diverse human tumour types. Nature 1989;342:705–8.
24. Hockenbery D, Nunez G, Milliman C, Schreiber RD, Korsmeyer SJ. Bcl-2 is an inner mitochondrial membrane protein that blocks programmed cell death. Nature 1990;348:334–6.
25. Carson WE, Haldar S, Baiocchi RA, Croce CM, Caligiuri MA. The c-kit ligand suppresses apoptosis of human natural killer cells through the upregulation of bcl-2. Proc Natl Acad Sci U S A 1994;91:7553–7.
26. Pan G, Vickers SM, Pickens A, et al. Apoptosis and tumorigenesis in human cholangiocarcinoma cells. Involvement of Fas/APO-1 (CD95) and calmodulin. Am J Pathol 1999;155:193–20.
27. Li-Weber M, Giaisi M, Baumann S, Treiber MK, Krammer PH. The anti-inflammatory sesquiterpene lactone parthenolide suppresses CD95-mediated activation-induced-cell-death in T-cells. Cell Death Differ 2002;9: 1256–65.
28. Biswas RS, Cha HJ, Hardwick JM, Srivastava RK. Inhibition of drug-induced Fas ligand transcription and apoptosis by Bcl-XL. Mol Cell Biochem 2001;225:7–20.
29. Zhang S, Ong CN, Shen HM. Involvement of proapoptotic Bcl-2 family members in parthenolide-induced mitochondrial dysfunction and apoptosis. Cancer Lett 2004;211:175–88.
30. Antonsson B, Montessuit S, Sanchez B, Martinou JC. Bax is present as a high molecular weight oligomer/complex in the mitochondrial membrane of apoptotic cells. J Biol Chem 2001;276:11615–23.
31. Wei MC, Zong WX, Cheng EH, et al. Proapoptotic BAX and BAK: a requisite gateway to mitochondrial dysfunction and death. Science 2001;292:727–30.
32. Saito M, Korsmeyer SJ, Schlesinger PH. BAX-dependent transport of cytochrome *c* reconstituted in pure liposomes. Nat Cell Biol 2000;2:553–5.
33. You KR, Wen J, Lee ST, Kim DG. Cytochrome *c* oxidase subunit III: a molecular marker for *N*-(4-hydroxyphenyl)retinamise-induced oxidative stress in hepatoma cells. J Biol Chem 2002;277:3870–7.
34. Wolter KG, Hsu YT, Smith CL, Nechushtan A, Xi XG, Youle RJ. Movement of Bax from the cytosol to mitochondria during apoptosis. J Cell Biol 1997;139: 1281–92.
35. Narita M, Shimizu S, Ito T, et al. Bax interacts with the permeability transition pore to induce permeability transition and cytochrome *c* release in isolated mitochondria. Proc Natl Acad Sci U S A 1998;95:14681–6.
36. Mikhailov V, Mikhailova M, Degenhardt K, Venkatachalam MA, White E, Saikumar P. Association of Bax and Bak homo-oligomers in mitochondria. Bax requirement for Bak reorganization and cytochrome *c* release. J Biol Chem 2003;278:5367–76.
37. Bojes HK, Datta K, Xu J, et al. Bcl-xL overexpression attenuates glutathione depletion in FL5.12 cells following interleukin-3 withdrawal. Biochem J 1997;325:315–9.
38. Friesen C, Herr I, Krammer PH, Debatin KM. Involvement of the CD95 (APO-1/FAS) receptor/ligand system in drug-induced apoptosis in leukemia cells. Nat Med 1996;12:574–7.
39. Müller M, Strand S, Hug H, et al. Drug-induced apoptosis in hepatoma cells is mediated by the CD95 (APO-1/Fas) receptor/ligand system and involves activation of wild-type p53. J Clin Invest 1997;99:403–13.
40. Fulda S, Sieverts H, Friesen C, Herr I, Debatin KM. The CD95 (APO-1/Fas) system mediates drug-induced apoptosis in neuroblastoma cells. Cancer Res 1997; 57:3823–9.
41. Goping IS, Gross A, Lavoie JN, et al. Regulated targeting of BAX to mitochondria. J Cell Biol 1998; 143:207–15.
42. Griffiths GJ, Dubrez L, Morgan CP, et al. Cell damage-induced conformational changes of the pro-apoptotic protein Bak *in vivo* precede the onset of apoptosis. J Cell Biol 1999;144:903–14.
43. Marzo I, Brenner C, Zamzami N, et al. Bax and adenine nucleotide translocator cooperate in the mitochondrial control of apoptosis. Science 1998;281:2027–31.
44. Picman AK, Rodriguez E, Towers GH. Formation of adducts of parthenin and related sesquiterpene lactones with cysteine and glutathione. Chem Biol Interact 1979; 28:83–9.
45. Woerdenbag HJ, Lemstra W, Malingre TM, Konings AW. Enhanced cytostatic activity of the sesquiterpene lactone eupatoriopicrin by glutathione depletion. Br J Cancer 1989;59:68–75.